Aeolian Research 1 (2010) 147–153

Contents lists available at ScienceDirect

Aeolian Research

journal homepage: www.elsevier.com/locate/aeolia

Estimating the saltation and suspension components from field wind erosion ☆

L.J. Hagen [a,*], S. van Pelt [b,1], B. Sharratt [c,2]

[a] USDA-ARS, GMPRC, 1515 College Avenue, Manhattan, KS 66502, USA
[b] USDA-ARS, 302 W IH 20, Big Spring, TX 79720-0013, USA
[c] USDA-ARS, 213 LJ Smith Hall, Washington State University, Pullman, WA 99164, USA

ARTICLE INFO

Article history:
Received 24 October 2008
Revised 20 August 2009
Accepted 25 August 2009

Keywords:
Wind erosion
Dust
Saltation

ABSTRACT

Improving wind erosion prediction and control requires correct estimates of the suspended dust (ss) and saltation (sn) components from field erosion events. The objectives of this study were to (a) develop an improved methodology (HPS) to estimate the fractions of sn and ss in the sediment discharge, and (b) compare HPS predictions to those of LM (Leys and McTainsh, 1996) and CN (Chepil and Woodruff, 1978; Nickling, 1978) that included or FS (Fryrear and Saleh, 1993) that excluded size measurements of the trapped sediment. Sediment flux profiles from nine field studies in four states were used in the data analyses. The log form of the ss flux profile developed in the LM method for dispersed particles had poor data fit to profiles of aggregated particles. The FS, HPS, and CN methods predicted significantly different ratios of ss discharge to total discharge in the order FS < HPS < CN. The widely-used power form of the ss flux profile in the CN method provided a good data fit above 0.1 m, but over estimated ss flux near the surface. The FS method over estimated sn and under estimated ss components. The HPS method obtained good fits to the data, even when profile gradients were large. Thus, using the sieved sediment catch from passive sediment catchers coupled with HPS analysis methodology offered significant improvements in the accuracy of estimates of sn and ss discharge. On short fields, the fraction of ss discharge was related to soil texture.

Published by Elsevier B.V.

1. Introduction

Wind erosion is a major conservation problem in arid and semiarid regions around the world that support about one-sixth of the world's population (Skidmore, 2000). Wind erosion is caused by inadequately protecting soil against wind shear. A lack of vegetative cover to protect the soil surface against wind shear is problematic in arid and semiarid regions because of low precipitation and high evaporation rates. However, soil aggregation, crusting, soil moisture, and humidity also may reduce erosion. Wind erosion occurs across a range of landscapes including playa lakes (Cahill et al., 1996), cropland (Zobeck and van Pelt, 2006), shrubland (Whicker et al., 2002), forest (Whicker et al., 2006) and desert (Honda and Shimizu, 1997). Wind erosion sorts the most fertile fraction from the soil and lowers its productivity, deposits sediment in ditches and waterways, pollutes the air, reduces visibility, and fouls machinery.

To facilitate prediction and control of wind erosion, as well as validate models, improved methods are needed to estimate the partitioning of the eroding soil discharge between the saltation (sn) and suspension (ss) components of wind erosion transport trapped in catchers.

Saltation (defined here as aggregates >106 μm diameter hopping across the soil surface) abrades immobile surface clods and crusts to create both additional suspension-size (<106 μm diameter) and saltation/creep aggregates. Aggregates in sn also break down to provide additional ss-size aggregates (Hagen, 2002; Mirzamostafa et al., 1998). The portion of the eroding soil discharge moving in sn has a significant effect on erodibility of downwind field surfaces and, thus, the predicted erosion (Hagen, 2008). The sn discharge is also used as a major factor in generating PM10 (particulate matter <10 μm aerodynamic diameter) (Ono, 2006; Zobeck and van Pelt, 2006) and dust emissions (Shao, 2001; Hagen et al., 1999). The wind transport capacity for ss sediment far exceeds that for sn sediment. Hence, on large eroding surfaces the fraction of sediment transported in ss typically increases downwind and may easily exceed that in sn (Gillette et al., 1997). The erosion control measures needed for surfaces dominated by sn or ss discharge also differ. For example, tillage ridges on soils are effective

☆ Contribution from USDA, ARS in cooperation with Kansas Agricultural Experiment Station. Contribution No. 09-065-J from the Kansas Agricultural Experiment Station, Manhattan, KS.

* Corresponding author. Address: USDA-ARS, GMPRC, Wind Erosion Lab, 1515 College Avenue, Manhattan, KS 66502, USA. Tel.: +1 785 539 5545.
E-mail addresses: hagen@weru.ksu.edu (L.J. Hagen), scott.vanpelt@ars.usda.gov (S. van Pelt), brenton.sharratt@ars.usda.gov (B. Sharratt).
[1] Tel.: +1 432 263 0293.
[2] Tel.: +1 509 335 2724.

1875-9637/$ - see front matter Published by Elsevier B.V.
doi:10.1016/j.aeolia.2009.08.002

at trapping sn aggregates but may not reduce erosion rates on soils composed mainly of ss-size aggregates during high winds.

Soil eroded by wind is commonly measured using passive sediment catchers (Zobeck et al., 2003). Although passive sediment catchers vary in their design, all operate by trapping sn and/or ss material as airstreams move through the catcher. Catchers have been designed to trap sediment in the airstream within the sn layer, effectively integrating from the soil surface to about 0.5 m above the soil (Nickling and McKeena-Neuman, 1997). Most catchers, however, are constructed to sample at discrete heights above the soil surface (Zobeck et al., 2003). Catchers that sample at discrete heights have the advantage of ascertaining the vertical profile in sediment moving across a landscape.

The amount of ss sediment passing a point is often calculated by measuring the mass of ss-size sediments trapped at various heights, fitting an equation to these point measurements, and then integrating the equation from near the surface upwards to estimate the ss discharge for a given period. To describe the vertical profiles of ss sediment flux, various forms of fitting equations have been proposed. Leys and McTainsh (1996) used the form (hereafter called LM)

$$F_{ss} = t + v\log(Z) \tag{1}$$

to fit ss mass flux of fully dispersed particulates <90 μm in diameter.

While the most popular is a power equation of the form

$$F_{ss} = aZ^{p} \tag{2}$$

used by Chepil and Woodruff (1978) and Nickling (1978) (hereafter called CN), where F_{ss} is flux of ss-size sediment moving horizontally (kg m^{-2}); Z, height above the surface (m); and a, p, t, and v are fitting coefficients.

The preceding profile equations do not fit at zero height, but are often assumed to fit near the soil surface, so an arbitrary lower integration height (Z_1), such as 0.001 m, was selected. However, the estimated ss discharge is sensitive to both the assumed profile form near the surface as well as the selected Z_1, but these generally have not been validated.

To eliminate the labor and equipment necessary to measure the size distribution of the trapped sediments, Fryrear and Saleh (1993) proposed an alternative methodology (hereafter called FS), to estimate the proportions of sn and ss sediment using the horizontal flux of all sediment collected by catchers installed at various heights above the surface (Fryrear, 1986). The FS methodology has not been validated by measured data.

The objectives of this study were to (a) develop an improved methodology (hereafter called HPS) to estimate the proportions of sn and ss aggregates in the sediment discharge based on sieve cuts of the trapped sediments, and (b) compare the HPS results to those using LM, FS and CN methodologies.

2. Methods and materials

Considerable wind erosion data are available from field experiments collected using passive sediment catchers (Fryrear et al., 1991; Zobeck et al., 2003). Typically, point measurements of horizontal sediment flux are collected with catchers placed at heights of about 0.05, 0.1, 0.2, 0.5 and 1.0 m above the soil surface. Fitting curves to the horizontal flux measurements and integrating these over height provides an estimate of the total horizontal sediment discharge at a point in the field. Typically, these data are used to estimate field soil loss (Fryrear and Saleh, 1993; Sharratt et al., 2007; Hagen, 2004). Subsets of these field data were used in the present study to estimate the sn and ss fractions of eroding soil discharge.

2.1. Field wind erosion flux data

One set of field results that includes both the near-surface fluxes along with sieved sediment catch data was reported from the "Wolfforth field experiment" (Stout and Zobeck, 1996). In this experiment, wind erosion was measured on an agricultural field in Texas soon after sowing the field to wheat in early spring. Eight sampling heights of flux data were collected at 0.0013, 0.0059, 0.015, 0.045, 0.095, 0.245, 0.695 and 1.645 m above the surface. To match our sieve cuts at other field sites, the sieved Wolfforth catch data were linearly interpolated to determine the fraction <106 μm. These data were then used as a test of the HPS methodology developed in this study as well as prior methodology in the literature.

Sediment catch samples were obtained at an additional five agricultural field sites located in Colorado, Kansas, Texas, and Washington. These sites varied in soil texture and surface characteristics at the time of the erosion events (Table 1). Sediment catch profiles from eight erosion events at these locations were sieved with micromesh sieves (ATM Corp., Milwaukee, WI[3]) with 250, 106, 53 and 10 μm openings. The surface conditions and soil losses from each storm event are reported in Table 2.

2.2. Data analysis methodologies

Using four methodologies, estimates of the ss and sn discharge for each profile were developed from the trapped sediment data.

2.2.1. LM and CN methodologies

Based on the methods used in prior research by Leys and McTainsh (1996) and Nickling (1978) two estimates were developed by fitting profile flux equations (Eqs. (1) and (2)) to the sieved ss flux data. The data were fitted from 0.1 to 1.0 m, except for the Wolfforth profile which was fitted from 0.095 to 1.645 m. The ss profiles below 0.1 m were assumed to be described by the same equation parameters. The ss discharge was then estimated by integrating these fitted equations from 0.001 to 2.0 m, except the Wolfforth profile which was integrated to 1.645 m.

2.2.2. FS methodology

Another set of estimates of the ss and sn fractions was developed from total sediment flux profiles using FS methodology (Fryrear and Saleh, 1993). In the FS method, sediments in the three catchers nearest the soil surface (ca. 0.05, 0.10, and 0.2 m height) were fitted to an exponential equation

$$F_{sn} = b\exp(cZ) \tag{3}$$

where F_{sn} is near-surface horizontal sediment flux for erosion event (kg m^{-2}); Z, height above the soil surface (m); and b, c are regression fitting coefficients.

Sediments in the three highest catchers (ca. 0.2, 0.5, 1.0 m height) were fitted to the power equation (Eq. (2)).

Next, a transition height between sn and ss (TSS height) was calculated as the highest height at which the fluxes predicted by Eqs. (2) and (3) were equal or nearest equal. Eq. (3) was then integrated from the surface to the TSS height and designated the sn discharge, whereas Eq. (2) was integrated from the TSS height to about 2.0 m and designated the ss discharge.

2.2.3. HPS methodology

A final set of calculated sn and ss discharge estimates were developed using a new methodology, called HPS. The HPS methodology

[3] Mention of trade names or commercial products in the article is solely for the purpose of providing specific information and does not imply recommendation or endorsement by the US Department of Agriculture.

Table 1
Test sites and surface soil intrinsic properties.

Location	Soil texture	Sand (%)	Silt (%)	Clay (%)	Very fine sand (%)	Organic matter (%)
Wolfforth, Texas	Fine sandy loam	73.5	11.4	15.1	Est[a] 18	0.34
Big Spring, Texas	Loamy sand	83.6	8.4	8.0	21.2	0.3
Elkhart, Kansas	Sandy loam	68.1	21.5	10.4	12.9	0.7
Eads, Colorado	Clay loam	29.3	38.6	32.1	16.3	1.6
Washtucna, 1 Washington	Silt loam	30	63	7	20	1.6
Washtucna, 2 Washington	Silt loam	40	53	7	15	1.5

[a] Est = estimated.

attempts to account for the complex curvature of the ss flux profile as it approaches the surface.

In the HPS procedure, an equation recommended by Stout and Zobeck (1996) was fitted to the sn flux data as

$$q_{sn} = \frac{f}{\left(1 + \frac{Z}{s}\right)^h} \tag{4}$$

and integrated from the surface to 1.0 m height as

$$Q_{sn} = \int_0^{1.0} q_{sn}\, dZ \tag{5}$$

where Q_{sn} is sn discharge (kg m^{-1}); Z, height above the soil surface (m); and f, h, and s are regression fitting coefficients.

The preceding equation provides a more flexible fit to the sn data, because it has three fitting coefficients compared to two in the exponential form (Eq. (3)) often used to fit sand discharge measurements (Vories and Fryrear, 1991). When sn flux measurements are not available at 0.05 m or lower, however, Eq. (4) may trend toward infinite flux estimates near the surface. In this case, Eq. (3) should be used to reduce the possibility of large errors in fitting the data.

The ss-size sediment discharge is often fitted by a power-law expression (Eq. (2)) with a negative exponent. It becomes infinite approaching the soil surface, however, so the aerodynamic roughness is sometimes used as a lower limit. For analyzing the ss component from sediment catchers in HPS, we propose using two equations. First, integrate the power-law using a lower limit of 0.1 m for both data fitting and integration

$$Q_{ss2} = \int_{0.1}^{2} aZ^p\, dZ \tag{6}$$

where Q_{ss2} is upper ss discharge (kg m^{-1}); Z, height above the soil surface; and a, p are regression coefficients.

As discussed later, other factors besides diffusion influence the ss profiles below the 0.1 m height. Hence, fit hyperbolic and exponential equations to the lower portion of the ss flux data and select the one with the highest R^2. Finally, integrate the selected equation from the surface to 0.1 m. The hyperbolic flux equation has the form

$$qss1_h = \frac{jm}{m + Z} \tag{7}$$

and integrated is

$$Q_{ss1} = \int_0^{0.1} qss1_h\, dZ \tag{8}$$

where Q_{ss1} is lower ss discharge (kg m^{-1}), and j, m are regression fitting coefficients.

Alternatively, the exponential equation (Eq. (3)) with different coefficients can be used for the lower ss flux and integrated to estimate the discharge as

$$Q_{ss1} = \int_0^{0.1} b \exp(cZ)\, dZ \tag{9}$$

where b and c are regression fitting coefficients.

Summing Q_{ss2} and the selected Q_{ss1} gives the total measured ss discharge (Q_{ss}).

Fitting equation (3) and (7) require estimating a third ss flux data point near the surface along with the data from 0.05 and 0.10 m heights that are often available.

The ss flux at 0.001 m above the surface was calculated by multiplying the sn flux at 0.001 m (calculated using Eq. (3)) by an estimate of the fraction of ss component at 0.001 m relative to the sn sediment flux as

$$q_{ss} = q_{sn} \frac{SF_{ss}}{1 - SF_{ss}} \tag{10}$$

Table 2
Storm dates, measured or estimated field surface conditions, and measured soil loss along field center strip.

Location and storm dates	Flat cover (fraction)	Aggregates <0.84 mm (fraction)	Crust cover (fraction)	Crust and aggregate stability[a] (Ln(J kg^{-1})	Random roughness (mm)	Ridge height (mm)	Soil loss (kg m^{-2})
Wolfforth							
April 14 1994	Field with damaged wheat seedlings and downwind gradients in surface conditions from prior emergency tillage and subsequent wind erosion						
Big Spring							
January 4, 1990	0.04	0.64	0.50	1.93	1.7	20	1.77
March 4, 1990	0.04	0.65	0.30	1.93	1.7	20	4.57
April 7, 1995	0.03	0.72	0.57	1.93	1.7	0	4.92
Elkhart							
April 10, 1991	0.10	0.37	0.50	2.47	5.4	45	0.81
March 8–9, 1992	0.10	0.70	0.46	2.47	3.0	0	7.47
Eads							
March 12, 1991	0.15	0.36	0.00	3.42	8.0	62	2.42
Washtucna 1							
September 25, 2001	0.4	0.84	0.00	No data	13	100	0.06
October 28, 2003	0.02	0.49	0.00	1.73	11	0	0.10

[a] Estimated from soil clay content.

where q_{ss} is estimated ss flux at 0.001 m height (kg m^{-2}); q_{sn}, estimated sn flux at 0.001 m height (kg m^{-2}); and SFss is estimated fraction of ss flux in total flux at 0.001 m height.

The fraction of ss component in the total flux was estimated as the lesser of the 0.05 m fraction or the 0.10 and 0.05 m fractions linearly extrapolated to the 0.001 m height.

The rationale for the preceding approach is that below about 0.05 m height, the high degree of mixing created by upward and downward moving sn-size aggregates coupled with 'splash' entrainment of the ss-size aggregates creates a relatively small vertical gradient in the fraction of ss-size aggregates in the total flux. After impact by sn, ss-size aggregates with diameters of 100, 75, 50 and 25 μm that leave the surface with an initial velocity of 5 m s^{-1} will have stopping distances of about 0.17, 0.047, 0.021 and 0.0053 m, respectively (Willeke and Baron, 1993). The aggregate stopping distance is directly proportional to the initial velocity and the square of the aggregate diameter. The splash and mixing processes cause entrainment of ss-size into the airstream, while the turbulent diffusivity (ε), as typically quantified, approaches zero near the surface (Kind, 1992).

$$\varepsilon = ku_*Z \tag{11}$$

where k is von Karman's constant (0.4); u^* is friction velocity (m s^{-1}); and Z is height above the soil surface (m).

All regression coefficients used in this study were determined using commercial software (SPSS Inc. 1997).

3. Results and discussion

3.1. Wolfforth experiment

Analysis of the profile of the Wolfforth sediment flux data, showed the 0.0013–0.095-m portion of the ss data was best fitted by the hyperbolic equation (Eq. (7)), whereas the 0.095–1.65-m ss data fit the conventional power equation (Eq. (2)), (Fig. 1).

Typically, flux data below 0.05 m are not available, so the HPS procedure was applied without the data below 0.05 m and compared to all data in the Wolfforth flux profile (Fig. 2). The results show a slight decrease in R^2 from 0.99 to 0.98 when using only part of the data to predict the ss fluxes. Hence, the HPS methodology for fitting the ss flux appears valid.

The profile sn flux data were fitted to Eq. (4) using both all the data and only the data at $\geqslant$0.045 m heights. In this case, all data were fitted with $R^2 = 0.92$ and the partial data set with $R^2 = 0.87$ (Fig. 3).

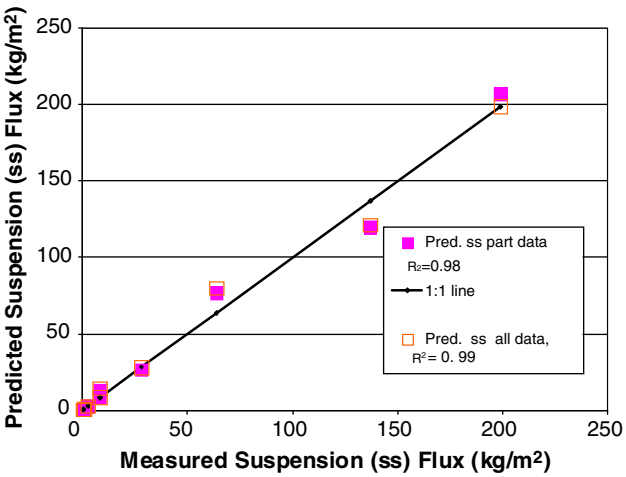

Fig. 2. Predicted (HPS) vs. measured Wolfforth suspension flux (ss) using all the measured profile data compared with predictions using part of the data. In the part data prediction, data from $\geqslant$0.095 m height were used in Eq. (2), and the 0.095–0.045 m data and a third estimated data point at 0.001 m were used in Eq. (7).

Estimating the flux moving near the surface is important, because 0.69 of sn and 0.63 of ss discharge passed below the 0.045 m height in the measured Wolfforth profile. The calculated ratio of ss discharge to total discharge (HPS Q_{ss}/Q_{tot}) using part of the data was 0.290 and using all data was 0.297. Hence, the HPS methodology using part of the data provided a close estimate of Q_{ss}/Q_{tot} for the Wolfforth flux profile.

In contrast, Q_{ss}/Q_{tot} for the LM method was 0.14 and CN was 0.35. The low Q_{ss}/Q_{tot} using the LM method was mainly caused by the poor profile fit of Eq. (1) to the Wolfforth data ($R^2 = 0.71$). The FS method Q_{ss}/Q_{tot} was 0.17 with a calculated TSS height of 0.095 m.

3.2. Suspension fraction in field experiments

We also compared the Q_{ss}/Q_{tot} obtained from an additional 32 sediment flux profiles in eight storms using the four methodologies.

Leys and McTainsh (1996) reported an excellent fit of Eq. (1) to measurements of an ss flux profile of dispersed particles in

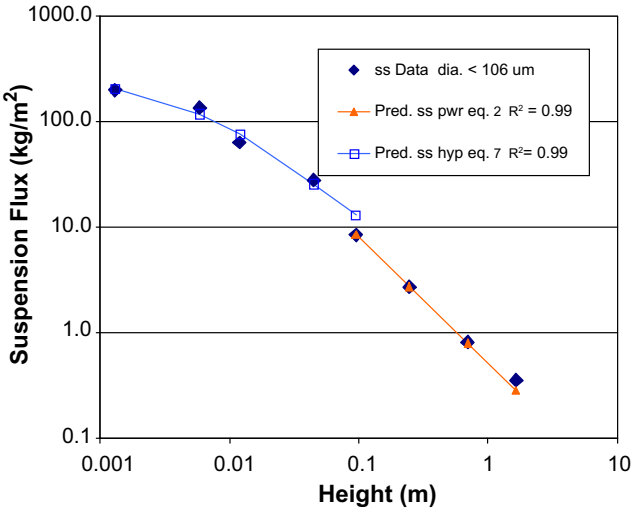

Fig. 1. Wolfforth suspension flux (ss) fitted to two curves (Eqs. (2) and (7)).

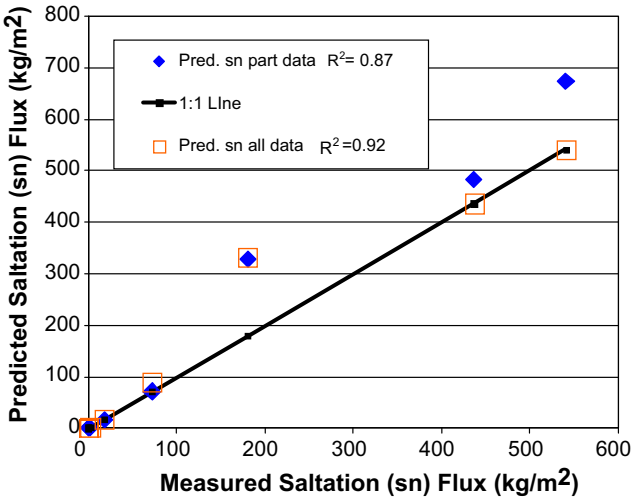

Fig. 3. Predicted (HPS) vs. measured Wolfforth saltation flux (sn), using all or part ($\geqslant$0.045 m height) of flux data in Eq. (3).

Australia. However, in this study, Eq. (1) fits the measured ss profiles of aggregates from 0.1 to 1.0 m with $R^2 = 0.73 \pm 0.16$, and often gave negative values of the ss flux when extrapolated to the 2 m height. When integrated to 1 m height, the result averaged 0.77 of the HPS values of Q_{ss}. Overall, Eq. (1) did not fit the profiles well and tended to underestimate the ss discharge in this data set. Hence, the mass flux ss profiles for dispersed and aggregated particles are best described by using different empirical equations.

For the six storms in the Great Plains, the means and standard deviations of Q_{ss}/Q_{tot} weighted by sediment discharge in the individual storms for the FS, HPS, and CN methods were 0.16 ± 0.12, 0.25 ± 0.06, and 0.48 ± 0.16, respectively. For the two storms on high silt soils at Washtucna, Washington the Q_{ss}/Q_{tot} for the FS, HPS, and CN methods were 0.61 ± 0.01, 0.95 ± 0.01, and 0.96 ± 0.01, respectively. A Kolmogorov–Smirnov test (Hollander and Wolfe, 1999) showed the Q_{ss}/Q_{tot} from FS, HPS and CN methods were significantly different ($P = 0.01$).

The power form of ss flux profile equation (2) used by Nickling (1978) and many others generally provided a good fit to the ss flux data above 0.1 m (average $R^2 = 0.96$), except at two profiles near the upwind non-erodible boundary. The CN method predicted that on average 69% of Q_{ss} was transported below 0.1 m height compared to 45% using HPS. The trends in predictions of Q_{ss}/Q_{tot} by the HPS and CN methods diverge when the coefficient p in Eq. (2) is less than about −1.3 (Fig. 4). In cases with steep gradients (Eq. (2) coefficient $p < -1.5$), the Q_{ss}/Q_{tot} is overestimated by the CN method. Including ss flux measurements near the surface (i.e., at 0.01–0.02 mm heights) could help mitigate the problem. Alternatively, restrict the CN method to profiles with modest gradients (i.e., Eq. (2), $p > -1.3$), where agreement with the HPS method was much improved.

By using Eq. (3) or (7) near the surface, the HPS method provided consistent predictions of Q_{ss}/Q_{tot} for profiles with large gradients.

Large vertical gradients often occur in eroding fields where both the sn and ss discharge are increasing along the downwind direction. For the six storms in the Great Plains, the measured sn discharge was increasing downwind, and none of these fields reached transport capacity (Fig. 5). A combination of small increases in downwind surface erodibility and insufficient field length prevented determination of the distance to transport capacity for these erosion events. Distance to maximum discharge in the

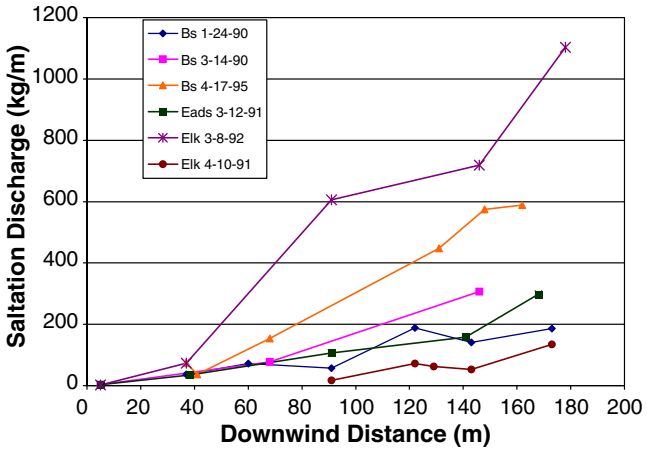

Fig. 5. Downwind saltation/creep discharge (HPS Q_{sn}) for six erosion events for various storm dates (BS = Big Spring, TX; Eads = Eads, CO; and Elk = Elkhart, KS).

Wolfforth experiment occurred at about 248 m downwind (Stout and Zobeck, 1996). Discharge variations with field length were not available from the Washtucna, Washington data which were averaged from several sediment catch clusters located near the downwind edge of the fields. The CN and HPS methods tended toward similar results at Wolfforth and Washtucna where the upwind fetch was about 250 m. To improve wind erosion models, additional data on distances to transport capacity of sn discharge are needed for a variety of soils and surface conditions.

The FS Q_{ss}/Q_{tot} data were reported by Fryrear (2000 a,b,c,d,e) or calculated from the flux data using FS methodology. In general, the FS Q_{ss}/Q_{tot} values tended to underestimate the HPS values (Fig. 6) over the entire range ($R^2 = 0.47$). There was a consistent correlation, however, between the HPS and FS Q_{ss}/Q_{tot} values ($R^2 = 0.79$). The TSS heights generally exceeded 0.2 m with a minimum of 0.08 m at Washtucna, Washington. The FS method overestimated the average sn discharge by 21%. The major merit of the FS method is that it eliminates the need determine the size distribution of the trapped sediment. But, the FS assumption that all discharge below a calculated height is composed of sn is clearly not correct, particularly for soils composed mainly of ss-size aggregates. Thus, for

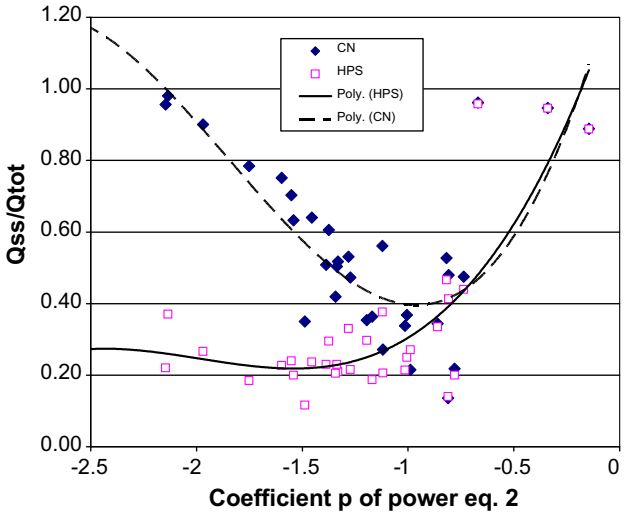

Fig. 4. Predicted CN and HPS Q_{ss}/Q_{tot} as a function of the coefficient p in power equation (2) fitted to ss flux profiles. Large negative p values denote large ss vertical gradients.

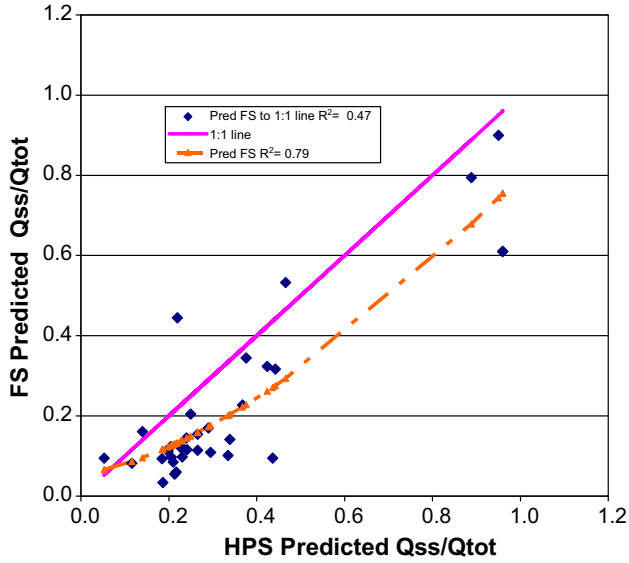

Fig. 6. Predicted FS vs. predicted HPS Q_{ss}/Q_{tot} for 34 flux profiles using data from nine erosion events at six locations.

accurate estimates of the sn and ss flux, it still appears necessary to determine the size distribution of the trapped sediment.

3.3. Soil texture effects on suspended soil fraction

The maximum fraction of ss-size (<106 μm in diameter) aggregates that can be created from the primary particles of a dispersed soil sample is the sum of the clay, silt and very fine sand fractions ($SFss_{max}$). Before the sn discharge reaches transport capacity, a relative measure of effectiveness in reducing eroding soil to ss-size during erosion is the ratio

$$R_f = \overline{(Q_{ss}/Q_{tot})}/SFss_{max} \quad (12)$$

where the overbar indicates the storm average fraction of ss discharge weighted by the total discharge. In this analysis, the lowest values of R_f were near 0.4 but increased as the clay, silt and very fine sand fraction increased (Fig. 7).

The R_f values greater than 1.0 occurred in two storms near Washtucna in eastern, Washington that had insignificant sn (1–10% of total discharge) and low total emissions (Table 2). In this case, the wind selectively enriched the ss component with additional fine aggregates that were not entirely representative of the surface soil composition.

4. Summary and conclusions

Four methodologies were tested to estimate the fraction of ss-size aggregates in the discharge of wind-eroded sediments.

The log form of the ss flux profile equation (1) suggested by Leys and McTainsh (1996) for dispersed particles did not provide good fits to the measured data using aggregated particles (average $R^2 = 0.73$) and often gave negative flux values when extrapolated to 2 m heights. When integrated with height, the LM method using Eq. (1), underestimated the ss discharge. Consequently, mass flux ss profiles for dispersed and aggregated particles are best fitted using different empirical equations.

The Q_{ss}/Q_{tot} predicted by the FS, HPS, and CN methods were significantly different ($P = 0.01$). For the six storms in the three Great Plains States, the Q_{ss}/Q_{tot} weighted averages predicted by the FS, HPS, and CN methods were 0.16, 0.25, and 0.48, respectively.

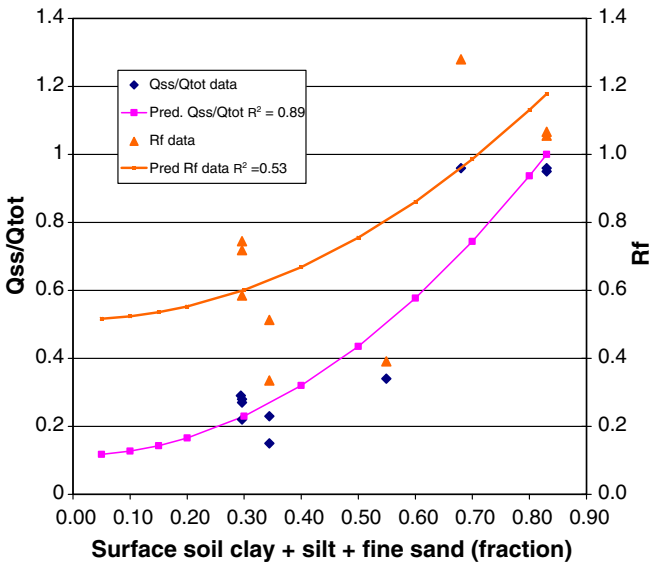

Fig. 7. Average R_f values for nine erosion events along with calculated weighted average HPS Q_{ss}/Q_{tot} values.

The power form of ss flux profile equation (2) used in the CN method (Nickling, 1978) generally provided a good fit to the ss flux data above 0.1 m (average $R^2 = 0.96$). When the profile gradients were large (i.e., Eq. (2) coefficient $p < -1.5$), however, the power equation tended to overestimate the ss flux when extrapolated downward toward the soil surface.

The FS method used total sediment flux collected in samplers to estimate the sn and ss discharge. Application of HPS methodology to sieved sn data showed average sn discharge was 21% less and ss discharge was 42% more than that calculated using FS methodology. Thus, using sieved sediment catch from passive catchers offers significant improvements in the accuracy of subsequent analysis to determine sn and ss discharge as well as downwind changes in sn discharge.

The HPS methodology developed in this study provided excellent fits to the flux profiles measured from 0.0013 to 1.645 m height reported for the Wolfforth field experiment. Overall, the Q_{ss}/Q_{tot} values predicted by HPS were significantly greater those from the LM and FS methods, but significantly less than those of the CN method, particularly for ss flux profiles with large vertical gradients.

Calculations of the sn discharge from six field sites showed that sn discharge increased downwind. The downwind increase in sn at these sites also increased vertical flux of ss and thus, contributed to the large vertical gradients in the measured ss flux. The HPS method improved accounting for variations in the ss flux near the surface and thus, provided satisfactory predictions of Q_{ss}/Q_{tot} values over the entire range of gradients in the ss flux profiles.

On average, the fraction of suspended soil in total discharge was well related ($R^2 = 0.89$) to the clay + silt + very fine sand fraction of the surface soil. This result is likely valid only where sn discharge is less than transport capacity, but may be useful for estimating Q_{ss}/Q_{tot} on short fields.

References

Cahill, T.A., Gill, T.E., Reid, J.S., Gearhart, E.A., Gillette, D.A., 1996. Saltating particles, playa crusts, and dust aerosols at Owens (Dry) Lake, California. Earth Surf. Process. Landforms 21, 621–639.

Chepil, W.S., Woodruff, N.P., 1978. Sedimentary characteristics of dust storms: II. Visibility and dust concentration. Am. J. Sci. 255, 104–114.

Fryrear, D.W., 1986. A field dust sampler. J. Soil Water Conserv. 41, 117–120.

Fryrear, D.W., 2000a. Wind Erosion Prediction System Validation: Elkhart Kansas. USDA-ARS, Big Spring, TX, Unpublished ARS Report.

Fryrear D.W., 2000b. Wind Erosion Prediction System Validation: Big Spring, 1989. USDA-ARS, Big Spring, TX, Unpublished ARS Report.

Fryrear, D.W., 2000c. Wind Erosion Prediction System Validation: Big Spring, 1995. USDA-ARS, Big Spring, TX, Unpublished ARS Report.

Fryrear, D.W., 2000d. Wind Erosion Prediction System Validation: Elkhart Kansas. USDA-ARS, Big Spring, TX, Unpublished ARS Report.

Fryrear, D.W., 2000e. Wind Erosion Prediction System Validation: Eads Colorado. USDA-ARS, Big Spring, TX, Unpublished ARS Report.

Fryrear, D.W., Saleh, A., 1993. Field wind erosion: vertical distribution. Soil Sci. 155 (4), 294–300.

Fryrear, D.W., Stout, J.E., Hagen, L.J., Vories, E.D., 1991. Wind erosion: field measurement and analysis. Trans. ASAE 34, 155–160.

Gillette, D.A., Fryrear, D.W., Xiao, J.B., Stockton, P., Ono, D., Helm, P.J., Gill, T.E., Ley, T., 1997. Large-scale variability of the wind erosion mass flux rates on Owens Lake 1. Vertical profiles of horizontal mass fluxes of wind-eroded particles with diameter greater than 50 μm. J. Geophys. Res. 102 (D22), 25977–25987.

Hagen, L.J., 2002. Processes of soil erosion by wind. Ann. Arid Zone 40 (3), 235–254.

Hagen, L.J., 2004. Evaluation of the Wind Erosion Prediction System (WEPS) erosion submodel on cropland fields. Environ. Softw. Model. 2, 171–176.

Hagen, L.J., 2008. Updating soil surface conditions during wind erosion events using the Wind Erosion Prediction System (WEPS). Trans. ASABE 51 (1), 129–137.

Hagen, L.J., Wagner, L.E., Skidmore, E.L., 1999. Analytical solutions and sensitivity analyses for sediment transport in WEPS. Trans. ASAE 42 (6), 1715–1721.

Hollander, M., Wolfe, W.A., 1999. Nonparametric Statistical Methods. Wiley, New York, NY.

Honda, M., Shimizu, H., 1997. Study of transport mechanism of Aeolian sediments from the Taklimakan Desert: implication of grain-size distribution and major-element composition. J. Arid Land Stud. 7, 139–146.

Kind, R.J., 1992. One-dimensional Aeolian suspension above beds of loose particles – a new concentration-profile equation. Atmos. Environ. 26A (5), 927–931.

Leys, J.F., McTainsh, G.H., 1996. Sediment fluxes and particle grain-size characteristics of wind-eroded sediments in southeastern Australia. Earth Surf. Process. Landforms 21, 661–671.
Mirzamostafa, N., Hagen, L.J., Stone, L.R., Skidmore, E.L., 1998. Soil and aggregate texture effects on suspension components from wind erosion. Soil Sci. Soc. Am. J. 62, 1351–1361.
Nickling, W.G., 1978. Eolian sediment transport during dust storms: Slims River Valley, Yukon Territory. Can. J. Earth Sci. 15, 1069–1084.
Nickling, W.G., McKeena-Neuman, C., 1997. Wind tunnel evaluation of a wedge-shaped Aeolian sediment trap. Geomorphology 18, 333–345.
Ono, D., 2006. Application of the Gillette model for windblown dust at Owens Lake, CA. Atmos. Environ. 40, 3011–3021.
Shao, Y., 2001. A model of mineral dust emissions. J. Geophys. Res. 106, 20239–20254.
Sharratt, B., Feng, G., Wendling, L., 2007. Loss of soil and PM10 from agricultural fields associated with high winds on the Columbia Plateau. Earth Surf. Process. Landforms 32, 621–630.
Skidmore, E.L., 2000. Air, soil, and water quality as influenced by wind erosion and strategies for mitigation. In: AGRONENVIRON 2000, Second International Symposium of New Technologies for Environmental Monitoring and Agro-Applications Proceedings, Tekirdag, Turkey, pp. 216–221.
SPSS Inc., 1997. Table Curve 2D Users Manual, Ver. 4, Chicago, IL.
Stout, J.E., Zobeck, T.M., 1996. The Wolfforth field experiment: a wind erosion study. Soil Sci. 161 (9), 616–632.
Vories, E.D., Fryrear, D.W., 1991. Vertical distribution of wind-eroded soil over a smooth, bare field. Trans. ASAE 34 (4), 1763–1768.
Whicker, J.J., Breshears, D.D., Wasiolek, P.T., Kirchner, T.B., Tavani, R.A., Schoep, D.A., Rodgers, J.C., 2002. Temporal and spatial variation of episodic wind erosion in unburned and burned semiarid shrubland. J. Environ. Qual. 31, 599–612.
Whicker, J.J., Pinder III, J.E., Beshears, D.D., 2006. Increased wind erosion from forest fire: implications for contaminant-related risks. J. Environ. Qual. 35, 468–478.
Willeke, K., Baron, P.A., 1993. Aerosol Measurement. Van Nostrand-Reinhold, New York.
Zobeck, T.M., van Pelt, R.S., 2006. Wind-induced dust generation and transport mechanics on a bare agricultural field. J. Hazard. Mater. 132, 26–38.
Zobeck, T.M., Sterk, G., Funk, R., Rajot, J.L., Stout, J.E., van Pelt, R.S., 2003. Measurement and data analysis methods for field-scale wind erosion studies and model validation. Earth Surf. Process. Landforms 28, 1163–1188.